PROCEEDINGS OF SCIENCE

BeX systems as seen by *INTEGRAL*

P. Blay,[a] A. Camero,[a] P. Connell,[a] P. Reig,[bc] S. Martínez-Nuñez,[d] and V. Reglero[a]

[a] *GACE - Image Processing Laboratory, University of Valencia*
PO BOX 22085, 46071, Valencia, Spain
[b] *IESL, FORTH*
711 10 Heraklion, Crete, Greece
[c] *Physics Department, University of Crete*
710 03 Heraklion, Crete, Creece
[d] *Dept. Física, Ing. De Sistemas y Teoría de la Señal, Universidad de Alicante*
03080 Alicante, Spain
E-mail: pere.blay@uv.es

We have analyzed data from all the BeX systems observed by *INTEGRAL* up to revolution 620. In addition, public data from other types of High Mass X-Ray Binaries (HMXRBs) was analyzed, with the goal to compare the temporal and spectral behavior of the BeX systems to those of other types of HMXRBs. As a result we show a very extensive temporal and spectral characterization work. Interesting conclusions about the different spectral behavior of BeX systems, when compared to other HMXRBs, will be presented and discussed. We find in the BeX systems a tendency to show harder spectra than those of Supergiant HMXRBs. Peculiar systems (i.e. 4U 2206+54, IGR J16138-4848, and IGR J163204751) clearly differ from the rest of HMXRBs.

7th INTEGRAL Workshop
September 8-11 2008
Copenhagen, Denmark

PoS(Integral08)078

1. The sample

The initial sample of BeXs is composed by 33 of such systems, all of them included in the *INTEGRAL*/ISGRI catalog (see [1]). They are shown in Table 1, together with their coordinates and known spin and orbital periods. We have analyzed, as well, a small subset of other types of HMXRBs, like systems including supergiant (SG) stars, peculiar systems or with unknown optical counterpart. They are shown in Table 2. They will serve, on the one hand, as test cases to be compared to the observed properties of the BeXs. On the other hand, for those with unknown optical counterpart, we will test the possibility to define to which group they will most likely belong (BeX or SG HMXRB). A representative of each of the newly defined classes of HMXRB (obscured sources and Super Fast X-ray Transients –SFXT–) have also been included, they are IGR J16318-4848 and IGR J17391-3021 respectively.

2. Light curves

Fig. 1 presents the *INTEGRAL*/ISGRI light curves of a subsample of sources showing one measurement per satellite pointing ($\sim$2-3 ks of integration time). We can differentiate two types of variability.

In the first kind (left column of Fig. 1), repeated short-outburst-like activity is shown over a long time span (on the order of $\sim$1000 days). We find every type of HMXRB showing this behavior (SG, SFXT and BeX systems). The difference between BeX and the rest of systems is the orbital periodicity of the type I outbursts, not present in the case of SG and SFXT, but this orbital periodicity can be be hidden by observational effects. Therefore, it is not possible to differentiate between classes of HMXRBs by only looking at the per-pointing light curve.

The other type of variability is that of the BeX systems shown in the right column of Fig. 1. These are systems showing type II outbursts, which happen on time scales on the order of $\sim$50 days. In this cases only BeX systems are found to show this type of variability in *INTEGRAL*/ISGRI data. The system with unknown counterpart, 4U 1901+03, shows this latter type of variability. Therefore, the data strongly suggests that this is a BeX system.

3. Indexes of variability

When comparing the percentage of observability (4th column of Table 3) (calculated comparing the number of pointings in which the source is detected to the total number of pointings with the source on the field of view) no distinction can be made between BeX and the other types of HMXRBs. If we take into account the amplitude of the variability (column 7 of 3) there seems to be a tendency in the BeX systems to have smaller amplitudes, but that result can be biased by the fact that in most of the detections of BeX systems the outbursts (type I or type II) have been observed only partially, and then the amplitude of the variability may not be reflecting a real value. Another factor to take into account is the time-span to which these data refers. The 8th column in Table 3 gives a factor over 100 which indicates the typical time-scale of the observation, with 100 corresponding to sources observed during most of the 5 years of data analyzed in this work. In general BeX systems show significantly lower time scale factor due to the fact that they are observed

Source	R.A. (deg)	DEC. (deg)	Pspin (s)	Porb (d)
IGR J01363+6610	24.02	66.17	-	-
RX J0146.9+6121	26.75	61.75	1412	-
IGR J01583+6713	29.58	67.22	-	-
V615 Cas	40.13	61.23	-	26.45
EXO 0331+530	53.75	53.17	4.4	34.3
X Per	58.85	31.05	837	250
1H 0521+373†	80.65	37.68	-	-
LMC X-3	84.73	-64.08	-	-
1A 0535+262	84.73	26.32	104	111
1H 0556+286	88.98	28.79	-	-
RX J0812.4-3114	123.12	-31.25	31.89	80
GRO J1008-57	152.45	-42.81	93.54	155
4U 1036-56	159.39	-56.8	-	-
1A 1118-615	170.24	-61.92	405	-
IGR J11435-6109	176	-61.12	-	52.5
H 1145-619	177	-62.21	292.4	187.5
PSR B1259-63	195.75	16.41	0.05	1133
SAX J1324.4-6200	201.11	-62.01	170.84	-
H 1417-624	215.3	-62.7	17.6	42.2
SAX J1452.8-5949†	221.33	-59.83	437.4	-
H 1553-542†	239.46	-54.41	9.26	30.6
AX J1749.2-2725†	267.29	-27.42	220 ?	150
GRO J1750-27†	267.3	-26.65	4.45	29.8
AX J1820.5-1434	275.12	-14.57	152.26	-
3A 1845-024	282.07	-2.42	94.8	241
XTE J1858+034	284.68	3.44	221	-
XTE J1946+274†	296.41	27.37	15.8	80
KS 1947+300	297.4	30.21	18.7	40.43
EXO 2030+375	308.06	37.64	41.8	46
GRO J2058+42	314.75	41.72	198	110
SAX J2103.5+4545	315.9	45.75	358.6	12.68
Cep X-4	324.9	57.06	66.3	-

†Not classified completely unambiguously as BeX.

Table 1: Initial Sample of systems with Be star companion included in this work.

Source	Class	R.A. (deg)	DEC. (deg)	Pspin (s)	Porb (d)
3A 0114+650	SG	19.51	65.29	10008	11.59
3A 0726-260	?	112.22	-26.11	103.2	34.5
Ginga 0834-430	?	128.98	-43.19	12.3	110
IGR J16318-4848	SgB[e]?	247.95	-48.82	-	-
IGR J16320-4751	SG	248.01	-47.87	1300	8.96
IGR J17391-3021	SFXT	264.8	-30.34	-	-
4U 1807-10	?	272.68	-10.87	4.45	242.18
RX J1826.2-1450	SG	276.56	-14.85	-	4.1
Sct X-1	SG?	279.12	-7.61	112	-
XTE J1855-026	SG	283.88	-2.61	362	6.1
4U 1901+03	?	285.9	3.19	2.76	22.58
IGR J19140+0951	SG	288.52	9.88	-	-
3A 2206+543	MSD[1]	331.98	54.52	5560	9.5?

[1]Main Sequence Donor

Table 2: HMXRBs used to compare to those of the BeX sample.

only during outbursts, while the SG HMXRBs are known to be persistent sources and are expected to be detected more repeatedly. Not only one of the variability factors considered here, but the combination of them, provides an indication of the variability of the sources. Furthermore, in order to complete this analysis, comparison to *INTEGRAL*/ISGRI exposure maps should be taken into account.

4. Pulse periods

The pulse period analysis is still on going. However, for a few BeX systems, we have determined already the pulse period by using *INTEGRAL*/ISGRI data in the 20–40 keV energy range (see Table 4). For some of these sources (SAX J2103.5+4545, EXO 2030+375, 4U 0115+64, etc) the pulse period is known to suffer variations. The possibility to measure this variations with *INTEGRAL*/ISGRI data is still a work in development.

5. Color-flux diagrams

We have defined the soft color as:

$$\text{Soft Color (SC)} = \frac{40--60 \text{ kev Flux}}{20--40 \text{ kev Flux}}$$

By building the Color-Flux diagrams we find two types of behaviors. In the first case the soft color variation with flux is quite linear, as shown in the plots of the left column of Fig. 2. In the second case the sources draw a U-like curve in the Color-Flux diagram, as shown in the plots of the right column of Fig. 2. We find that the shape of the Color-Flux diagram will not help to

Source	Number of detections	N. of scws in the FOV	% Obs.	F^1_{av}	σ	Amp. Var. (%)	% of observability in 5 years
H 0115+634	62	751	0.08	54.5	2.3	4	0.087
EXO 0331+530	142	176	0.81	57	31	54	0.198
X Per	2	2	1.00	7.6	0.25	3	0.003
1A 0535+262	2	35	0.06	6.9	0.25	4	0.003
GRO J1008-57	60	777	0.08	4.2	1.2	29	0.084
H 1145-619	19	796	0.02	3.4	0.7	21	0.027
SAX J1324.4-6200	1	120	0.01	5.4	-	-	0.001
H 1417-624	7	513	0.01	5	1.7	34	0.010
AX J1749.2-2725	11	3276	0.00	4.1	1.1	27	0.015
XTE J1858+034	178	1308	0.14	9.9	4.4	44	0.248
KS 1947+300	49	345	0.14	7.8	2.6	33	0.068
EXO 2030+375	595	1271	0.47	65.2	7.9	12	0.830
SAX J2103.5+4545	183	855	0.21	4.7	1.4	30	0.255
3A 2206+543	16	160	0.10	4.6	1.4	30	0.022
3A 0114+650	104	652	0.16	4.5	2.5	56	0.145
XTE J1855-026	77	892	0.09	4.5	1.6	36	0.010
IGR J16320-4751	220	1254	0.18	34.5	2.4	7	0.307
IGR J19140+0951	81	1357	0.06	5.4	2.9	54	0.113
IGR J16318-4848	474	1297	0.37	7.0	5.0	71	0.661
4U 1901+03	570	1423	0.40	12	2	17	0.795
IGR J17391-3021	33	3286	0.01	7	4	57	0.046

[1]Average count rate in the 20-40 keV energy band.

Table 3: Number of detections of the subset of sources seen by *INTEGRAL*/ISGRI in the 20–40 keV energy band and indication of several variability indexes. The upper half of the table contains the BeX systems, in the lower half of the table, the rest of HMXRBs can be seen.

Source	P_{spin}	P_{orb}
4U 2206+54	5560 ± 10^a	9.5?
SAX J2103.5+4545	352 ± 5^b	12.68
KS 1947+300	18.7 ± 0.1	40.43
4U 0115+64	3.6146 ± 0.0001	24.3
EXO 2030+375	41.691798 ± 0.000016^c	46
X Per	835 ± 2	250

[a]see [4] [b]see [2] [c]see [3]

Table 4: Measurement of the spin period for a few BeX systems with *INTEGRAL*/ISGRI data in the 20-40 keV energy range.

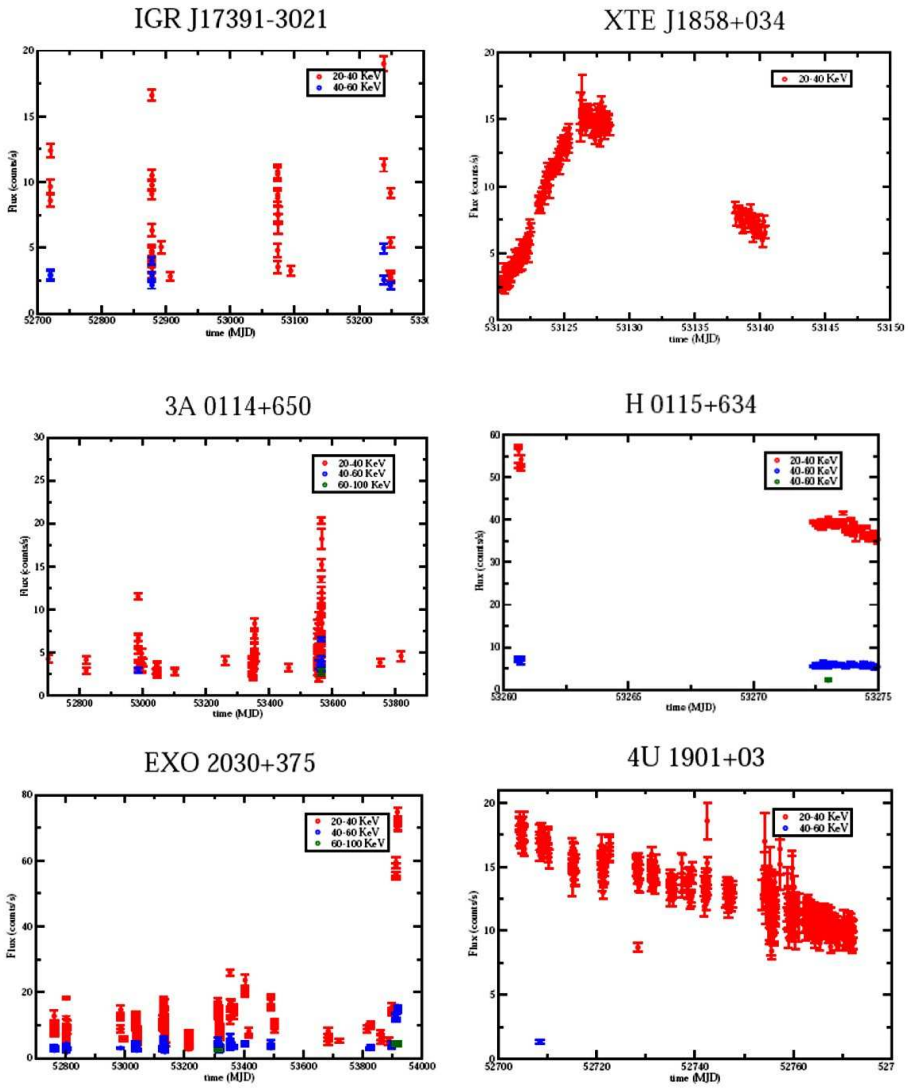

Figure 1: Left column: Long time span light curves (∼1000 days). **Right column:** Short time span light curves (∼20–50 days), including that of the system 4U 1901+03 with unknown counterpart.

characterize the BeX system nor to differentiate between types of HMXRB systems. The shape of the Color-Flux curve is independent of the nature of the source.

6. Spectral characterization

As seen in Table 5, spectra for most of the detected sources have been extracted in the 20–100 keV energy range. In order to allow for comparison, the same spectral model have been used to fit all the spectra. A simple powerlaw have been used, modified by a cutoff whenever the powerlaw by itself could not yield a good fit. For those sources showing spectral absorption features (like Cyclotron Scattering Resonant Features), gaussians in absorption have been used to help obtaining

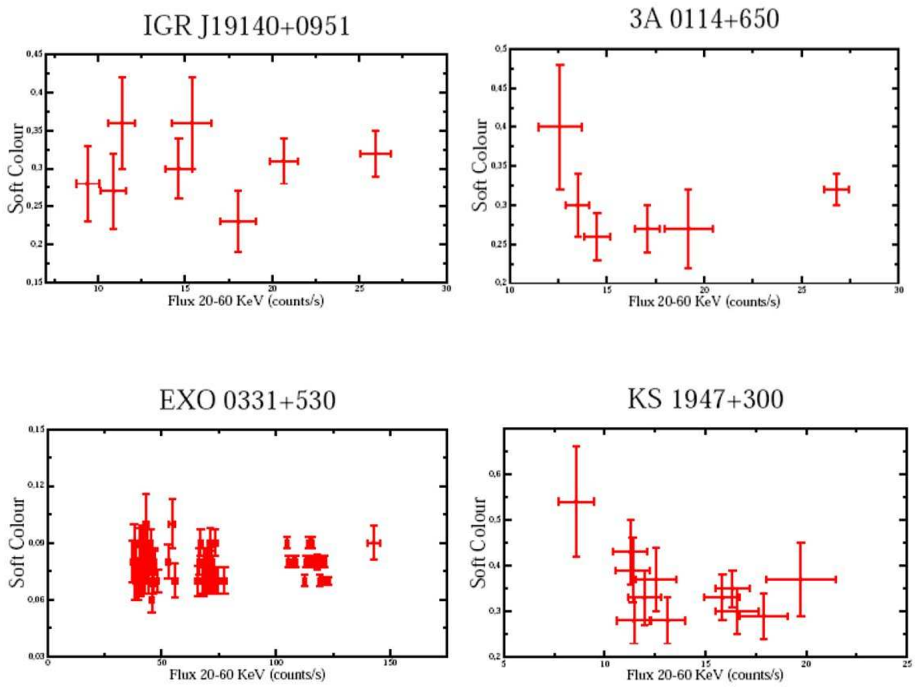

Figure 2: Left Column: Example of Color-Flux plot for those sources showing a linear behavior **Right Column:** Example of Color-Flux plot for those sources showing a U-like behavior.

a good continuum fit. Our goal is not to analyze the details of the spectral features, but to compare the continuum, that is, the spectral shape, with the aim to check for systematic differences between types of HMXRBs. We can stress out two clearly visible tendencies:

A) The BeX systems tend to have lower values of the photon index, while the SG systems all have values of the photon index above 2.5.

B) The BeX systems admit a cutoff as improvement of the spectral fit, however the wind-fed systems (SG HMXRB plus the peculiar system 4U 2206+54) will not admit a cutoff in the spectral fit.

The suggestion that systematic differences in the spectral shape are reflecting the mechanism of mass transfer present in the system is strong. We have added to our set two sources with SG companions but in which the accretion is mediated by an accretion disk, as happens in the BeX systems. This is the case of Cyg X-1 and SMC X-1 (shown in Table 5). These two systems present a photon index similar to that of the BeX system and also admit the addition of a cutoff to the spectral fit. As expected, the accretion mechanism present in the system strongly affects the shape of the spectrum of the source.

7. Conclusions

We have developed an extensive analysis of 5 years of *INTEGRAL*/ISGRI data of the BeX systems included in the ISGRI catalog, as well as a few SG HMXRBs. We have seen that regarding

Source	Γ	Ecut	Efold	χ^2_{red}	DOF	gabs
XTE J1858+034	0.8^{+1}_{-3}	22^{+2}_{-4}	8^{+4}_{-4}	1.4	13	
EXO 0331+530	$1.3^{+1.0}_{-1.0}$	32^{-2}_{+2}	7^{-2}_{+2}	1.3	11	$29^{+0.2}_{-0.2}$,50^{+1}_{-1},60^{+1}_{-1}
Cyg X-1[a]	1.5^{+1}_{-1}	175^{+40}_{-41}				
SMC X-1[b]	$1.5^{+0^{9}}_{-0.8}$	24^{+2}_{-2}		1.1	17	
SAX J2103.5+4545	$1.7^{+0.6}_{-0.5}$	26^{+8}_{-5}	38^{+36}_{-12} 0.9	45		
X Per	$1.8^{+0.2}_{-0.2}$			1.1	47	
KS 1947+300	$2.2^{+0.2}_{-0.2}$	57^{+6}_{-6}	23_7^{+7}	1.5	20	
IGR J19140+0951	$2.32^{+0.08}_{-0.11}$	52^{+5}_{-8}	56^{+11}_{-11}	1.3	20	
4U 1901+03	$2.4^{+0.6}_{-1.2}$	$24.9^{+0.4}_{-0.6}$	12^{-2}_{+2}	1.8	20	
EXO 2030+375	$2.5^{+0.2}_{-0.1}$			1.2	24	
IGR J17391-3021	$2.57^{+0.09}_{-0.11}$					
3A 0114+650	$2.6^{+0.2}_{-0.2}$			1.02	13	45^{+6}_{-3},90^{+12}_{-25}
GRO J1008-57	$2.7^{+0.2}_{-0.2}$	43^{+14}_{-8}	10^{-2}_{+2}	0.6	20	
IGR J16318-4848[c]	$2.7^{+0.3}_{-0.3}$	43^{+4}_{-4}	26^{+6}_{-4}	0.6	3	
XTE J1855-026	$2.74^{+0.12}_{-0.11}$			1.9	22	
H 1145-619	$2.8^{+0.2}_{-0.2}$	45^{+50}_{-7}		1.7	15	70^{+5}_{-4}
H 0115+634	$2.88^{+0.05}_{-0.08}$	28^{+2}_{-1}	32^{+1}_{-1}	0.6	21	
3A 2206+543[c]	$3.1^{+0.8}_{-0.4}$			1.8	2	30^{+1}_{-4}
IGR J16320-4751[c]	$3.50^{+0.12}_{-0.11}$			1.8	5	

[a] Bouchet et al. 2003, A&A, 411,377

[b] Rev. 94-95

[c] From mosaic

Table 5: The *INTEGRAL*/ISGRI 20–100 keV spectra for some of the detected sources of our sample. Two SG systems with accretion driven by the presence of an accreting disk have been added to the sample, namely Cyg X-1 and SMC X-1.

to timing properties, only after a detailed analysis of the outburst properties the nature of the source can be suggested, but timing analysis is not conclusive by itself when considering count rates in a per-pointing basis. The patterns of variability are similar in terms of time-scale and amplitudes except for the case of BeX system showing only type II outbursts. In this case we propose the system 4U 1903+01 to be a BeX system, as the only *INTEGRAL*/ISGRI detection of the source shows the tail of an outburst very similar to that of the type II outbursts seen in BeX systems (as XTE 1858+035, or H 0115+63).

Spectral analysis presents itself as more promising in order to infer the physics of the accretion mechanism present in the system. We have seen that those system with an spectral photon index above 2.5 and which do not allow a cutoff in the spectral fit are very likely to be SG HMXRBs (win-fed systems). On the other hands systems with harder photon indexes and admitting a cutoff in their spectral fits will very likely be accreting via an accretion disk (they can be BeX systems or Roche-Overflow SG systems). This methodology seems to be promising in order to characterize the different types of HMXRBs, however an improvement in the spectral analysis (increased sensitivity

or more detections) is needed in order to reduce uncertainties and allow a better estimation of spectral parameters.

References

[1] Bird et al. 2007, ApJS, 170, 175

[2] Blay et al. 2004, A&A, 427, 293

[3] Camero et al. 2005, A&A, 441, 261

[4] Reig et al. 2008, in preparation